Guo-zheng Quan*, Zhen-yu Zou, Tong Wang, Bo Liu and Jun-chao Li

Modeling the Hot Deformation Behaviors of As-Extruded 7075 Aluminum Alloy by an Artificial Neural Network with Back-Propagation Algorithm

DOI 10.1515/htmp-2015-0108
Received April 25, 2015; accepted November 24, 2015

Abstract: In order to investigate the hot deformation behaviors of as-extruded 7075 aluminum alloy, the isothermal compressive tests were conducted at the temperatures of 573, 623, 673 and 723 K and the strain rates of 0.01, 0.1, 1 and 10 s^{-1} on a Gleeble 1500 thermo-mechanical simulator. The flow behaviors showing complex characteristics are sensitive to strain, strain rate and temperature. The effects of strain, temperature and strain rate on flow stress were analyzed and dynamic recrystallization (DRX)-type softening characteristics of the flow behaviors with single peak were identified. An artificial neural network (ANN) with back-propagation (BP) algorithm was developed to deal with the complex deformation behavior characteristics based on the experimental data. The performance of ANN model has been evaluated in terms of correlation coefficient (R) and average absolute relative error (AARE). A comparative study on Arrhenius-type constitutive equation and ANN model for as-extruded 7075 aluminum alloy was conducted. Finally, the ANN model was successfully applied to the development of processing map and implanted into finite element simulation. The results have sufficiently articulated that the well-trained ANN model with BP algorithm has excellent capability to deal with the complex flow behaviors of as-extruded 7075 aluminum alloy and has great application potentiality in hot deformation processes.

***Corresponding author: Guo-zheng Quan,** State Key Laboratory of Materials Processing and Die & Mould Technology, Huazhong University of Science and Technology, Hubei 430074; State Key Laboratory of Mechanical Transmission, School of Material Science and Engineering, Chongqing University, Chongqing 400044, China, E-mail: quangz3000@sina.com
Zhen-yu Zou, Tong Wang, State Key Laboratory of Mechanical Transmission, School of Material Science and Engineering, Chongqing University, Chongqing 400044, China
Bo Liu, Chongqing Changan Automobile Co., Ltd, Chongqing 400023, China
Jun-chao Li, State Key Laboratory of Mechanical Transmission, School of Material Science and Engineering, Chongqing University, Chongqing 400044, China

Keywords: 7075 aluminum alloy, constitutive model, artificial neural network, processing map, finite element simulation

Introduction

Aluminum alloys, with attractive combination of physical and mechanical properties, are widely considered as the optimal selection in the industry of automobile manufacturing, shipbuilding and aircraft manufacturing. As a typical aluminum alloy with high strength, 7075 alloy is extensively employed for various critical structural components due to its high strength/density ratio and reasonable high fracture toughness [1–4]. The hot deformation behaviors of metals, which are significantly affected by the deformation parameters involving strain, strain rate and temperature, make a great difference on the dimensional accuracy and mechanical properties of final products in the hot forming process. In the courses of plastic deformation under various conditions, several interconnected metallurgical phenomena including work hardening (WH) [5], dynamic recrystallization (DRX) [6] and dynamic recovery (DRV) [7] coexist with one being predominant. WH increases the flow stress of materials and reduces the plasticity, while softening phenomena like DRX or DRV decrease the flow stress and thereby restoring the ductility. The metallurgical phenomena and their interaction effects in the hot deformation condition issue in complex deformation behaviors. Consequently, the understanding of flow behavior at hot deformation condition is of great significance for the analysis of hot deformation processes and optimization of processing parameters.

In recent years, abundant efforts have been made to develop constitutive model by physical and mathematical simulative techniques to deal with complex flow behaviors of materials. At present, two types of constitutive models, namely analytical and phenomenological models, are in vogue for modeling hot flow behaviors of materials [8]. The analytical model is closely associated with physical theories, which means that this model

needs a very clear and deep understanding of flow behaviors and deformation mechanisms of metallic materials based on a large amount of experimental data. However, the phenomenological model, as the name says, is less rigorously related to physical theories and can be developed through limited amount of experimental data. The phenomenological model is widely adopted in practice for effective modeling of flow behaviors on account of its reasonable feasibility and availability in comparison with analytical model.

Typical phenomenological models are Arrhenius-type constitutive equations and constitutive model based on artificial neural network (ANN). The Arrhenius-type constitutive equations are obtained through regression analysis with experimental data. However, the low accuracy and poor flexibility of constitutive equation have made it ineffective in the characterization of complex constitutive relationship. Compared with constitutive equations, the ANN, as a relatively new artificial intelligence technique, is able to solve the highly complex problems well by simulating the behaviors of biological neural systems in computers. The typical structure of an ANN consists of one input layer, one output layer and one or more hidden layers that are connected by the fundamental units of ANN named artificial neurons with a function of taking a weighted sum of the inputs. The input layer receives input data and after processing it, sends them to the hidden layer. The hidden layer works as a complex network architecture to simulate the nonlinear relationships between input and output layers, processing the data calculation and sends a response to the output layer [9, 10]. The output layer accepts the response and produces the output result. This approach makes it possible to cope with the complex constitutive relationships between flow stress and processing parameters with a collection of representative examples obtained through a limited amount of experimental data from the desired mapping functions for training instead of a well-defined mathematical model [10–12].

A lot of research groups have been working on the description of constitutive relationships by ANN method for the past few years. Quan et al. developed an ANN model of as-cast Ti-6Al-2Zr-1Mo-1V alloy in a wide temperature range involving phase transformation [13] and predicted the high-temperature flow behaviors of 20MnNiMo alloy using ANN [14]. Lin et al. established the optimum hot forming processing parameters for 42CrMo steel based on ANN model [15]. Zhao et al. characterized the hot deformation of Ti600 titanium alloy using constitutive equations and ANN [16]. The results of these researches have demonstrated that ANN is an effective tool to model the nonlinear constitutive relationships.

In order to study the flow behaviors of as-extruded 7075 aluminum alloy, 16 compression tests were conducted at different temperatures and strain rates. The true strain–stress data collected in the compression tests were then employed to develop the ANN model. The evaluation of ANN model has been performed based on several statistical parameters. A three-dimensional (3D) response plot for the semi-continuous visualized description of the constitutive relationship was developed based on several groups of flow stresses at different strain rates and different temperatures in and out of experimental conditions predicted by the well-trained ANN model. Subsequently, a comparative analysis on the ANN model and the Arrhenius-type constitutive equation of as-extruded 7075 aluminum alloy developed by Quan et al. [17] have been conducted. The results indicate that the ANN model has better accuracy and it is a more excellent approach to model the flow behaviors of as-extruded 7075 aluminum alloy.

As the well-trained ANN model could provide a wider range of flow stress data, it can be applied to characterization of intrinsic hot workability and numerical simulation with high accuracy. Reddy et al. constructed processing maps based on predicted flow stresses by ANN model for Ti-6Al-4V alloy and demonstrated that ANNs can be effective for generating a more reliable processing map for industrial applications [18]. Quan et al. developed an ANN model for 42CrMo high strength steel and improved the accuracy of finite element method (FEM) simulation by importing a wide range of flow stress curves predicted by the ANN model [19]. In the current work, the well-trained ANN model for as-extruded 7075 aluminum alloy was successfully applied to construct processing map and incorporated into numerical simulation by using FEM on Deform software, indicating that the application potentiality of ANN model in hot deformation processes is great.

Materials and experimental procedure

The chemical compositions of as-extruded 7075 aluminum alloy (Al-Zn-Mg-Cu) employed in this study is as follows (wt %): Zn-5.5, Mg-2.2, Cr-2.2, Cu-1.7, Si-0.4, Fe-0.3, Mn-0.1, Al (balance). The homogenized ingot was scalped to 16 cylindrical specimens with a diameter of 10 mm and a height of 12 mm. Before compression

tests, two thermocouple wires, i. e. two dissimilar conductors, were welded on two spots with a distance of 1 mm at the mid-span of each billet where a temperature differential is experienced by the two different conductors. In the following, the specimens were placed in a computer-controlled servohydraulic Gleeble 1500 thermomechanical simulator, and then resistance heated at a heating rate of 5 K/s and held at a fixed temperature for 180 s by thermo-coupled feedback-controlled AC current, which decreased the material anisotropy in flow behaviors effectively. Next, all the 16 specimens were compressed to a fixed true strain of 0.9 (height reduction of 60 %) at four different temperatures of 573, 623, 673 and 723 K and four different strain rates of 0.01, 0.1, 1 and 10 s^{-1}.

During these compressions, the variations of nominal stress and nominal strain were monitored continuously by a personal computer equipped with an automatic data acquisition system during the compression process. The true stress and true strain were derived from the nominal data according to the following formula: $\sigma_T = \sigma_N(1-\varepsilon_N)$, $\varepsilon_T = \ln(1-\varepsilon_N)$, where σ_T is true stress, σ_N is nominal stress, ε_T is true strain and ε_N is nominal strain.

Results and discussion

Flow behavior characteristics of as-extruded 7075 aluminum alloy

The true stress–strain curves of as-extruded 7075 aluminum alloy compressed at different deformation conditions are shown in Figure 1. The flow stresses as well as the shapes of the flow curves are sensitively dependent on temperature, strain and strain rate. Comparing these curves with one another, it is found that the stress level decreases with temperature increasing or strain rate decreasing. This is induced by the fact that lower strain rate and higher temperature provide longer time for the energy accumulation and higher mobilities at boundaries that result in the nucleation and growth of dynamically recrystallized grains and dislocation annihilation [20, 21]. For all these 16 true stress–strain curves, following a rapid increase to a peak value, flow stress decreases with two different variation tendencies. At the compression conditions of 573–723 K and 0.01 s^{-1}, 623–723 K and

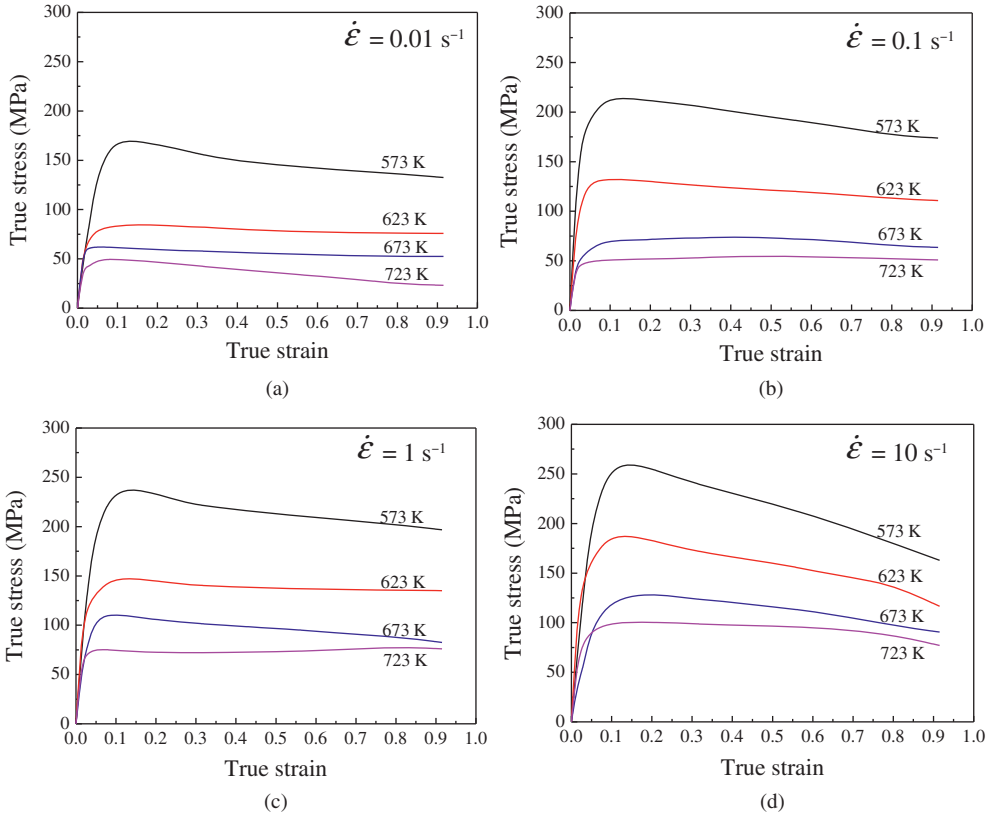

Figure 1: The true stress–strain curves of as-extruded 7075 aluminum alloy at different temperatures and the strain rates of (a) 0.01 s^{-1}, (b) 0.1 s^{-1}, (c) 1 s^{-1} and (d) 10 s^{-1}.

$0.1\,s^{-1}$, 623–723 K and $1\,s^{-1}$, and 723 K and $10\,s^{-1}$, flow stress decreases gradually to a steady state representing a balance between DRX softening and WH. At the compression conditions of 573 K and $0.1\,s^{-1}$, 573 K and $1\,s^{-1}$, and 573–623 K and $10\,s^{-1}$, flow stress decreases continuously, which indicates the sustainable development of DRX softening with an unbalance between DRX softening and WH. In summary, as for as-extruded 7075 aluminum alloy, the response of stress to the three deformation parameters including strain, strain rate and temperature shows highly nonlinear behaviors.

Development of ANN model for as-extruded 7075 aluminum alloy

ANN model

The back-propagation (BP) algorithm, one of the most popular learning algorithms for the multilayer feed-forward artificial neuron networks in materials modeling, was employed in this investigation to get a good understanding of the constitutive relationships between the inputs and outputs since it is a typical means of adjusting the weights and biases by utilizing gradient descent to minimize the target error [22] and it has a great representational power for dealing with complex and strongly coupled relationships [23].

The structure of ANN employed in the present work is schematically illustrated in Figure 2. The input variables in this investigation contain deformation temperature (T), strain (ε) and strain rate ($\dot{\varepsilon}$), while the output variable is flow stress (σ), as shown in Figure 2. In addition, two hidden layers were adopted to ensure the accuracy of ANN model. About 640 regular datasets have been extracted from the 16 stress–strain curves, in which the datasets at strain of 0.05, 0.1, 0.2, 0.3, 0.4, 0.5, 0.6, 0.7, 0.8 and 0.9 were selected for the purpose of modeling test, while the available datasets remained work as the training data. The experimental data involving temperature, strain, strain rate and stress must be normalized into dimensionless units before training, since these data were measured in different units, which results in the decrease of convergence speed and accuracy of the model. From the experimental data extracted from the stress–strain curves in Figure 1, it can be seen that the input strain data vary from 0.025 to 0.9, strain rate data vary from 0.01 to $10\,s^{-1}$, and the temperature data vary from 573 to 723 K, the output flow stress data vary from 23.1 to 264.971 MPa. The temperature data, strain data and the flow stress data were normalized within the range from 0.05 to 0.3 using the relation given by eq. (1). Meanwhile, the strain rate data, after taking logarithm of the values, were normalized using the relation given by eq. (2), since the range of the data is much too wide:

$$y_n = 0.05 + 0.25 \times \frac{y - 0.95y_{min}}{1.05y_{max} - 0.95y_{min}} \quad (1)$$

$$y_n = 0.05 + 0.25 \times \frac{(3+y) - 0.95(3+y_{min})}{1.05(3+y_{max}) - 0.95(3+y_{min})} \quad (2)$$

where y_n is the normalized value of y, y is the experimental data, y_{max} and y_{min} are the maximum and minimum values of y, respectively.

The structural parameters that are of great significance for an excellent ANN, i. e. hidden layer number, transfer function, training function and neuron number for each hidden layer, could make a big difference to the convergence speed and accuracy of the ANN model. In the present work, two hidden layers were adopted to ensure high accuracy. The functions “tan sigmoid” and “pure linear” were selected as the associated transfer function for each hidden layer and output layer, respectively. In addition, the training function is “trainbr.” As for the neuron number for each hidden layer, it was set by means of trial-and-error method according to the experience of designers and the training sample size. The ANN model may be insufficient to learn the process correctly when in training if the neuron number of each hidden layer is too small. On the contrary, too many neurons may slow down the convergence rates or over fit the data. As a result, the ANN model in current investigation was trained first with three neurons in each hidden layer, and then the neuron number was adjusted continually (from 3 to 18) for the purpose of getting a

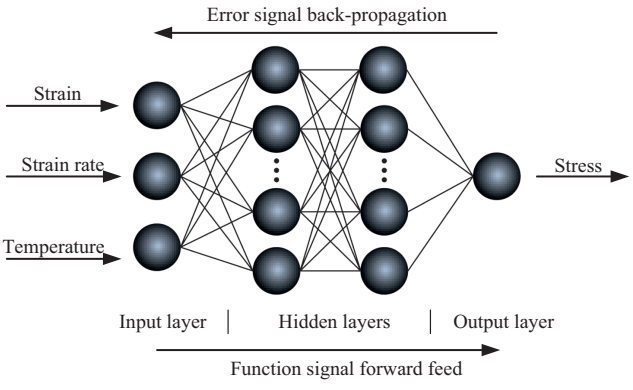

Figure 2: Schematic illustration of the artificial neural network architecture.

proper neuron number and approaching the expected accuracy.

Evaluation of the performance of the ANN model

During the training process of ANN model, the value of mean square error (MSE) is introduced to evaluate the ability of the ANN training work and determine the neuron number for each hidden layer, as expressed in eq. (3) [24]:

$$\mathrm{MSE} = \frac{1}{N}\sum_{i=1}^{N}(E_i - P_i)^2 \tag{3}$$

where E is the sample of experimental value, P is the sample of predicted value by ANN model and N is the number of strain–stress samples.

The MSE values were calculated after the accomplishment of each training process and recorded manually for different neuron numbers in each hidden layer. As a result, the MSE values of the different models are in the range of 0.1774–58.2675. In order to obviously display the small differences and variation trend with different neuron numbers, the MSE values were measured in logarithm, as shown in Figure 3. It is obviously seen that the MSE value decreases to the minimum value when the neuron number of each hidden layer is 14, showing that the ANN model with 14 neurons in each hidden layer exhibits excellent performance.

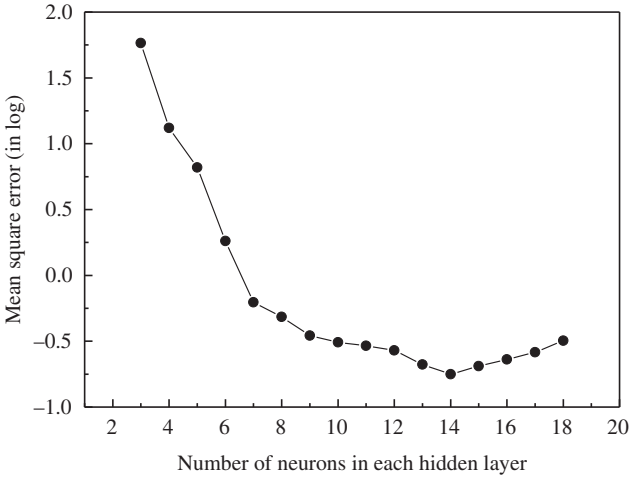

Figure 3: Performance of the network at different hidden neuron levels.

After the ANN model with 14 neurons in each hidden layer had been well developed, the performance was measured in terms of the correlation coefficient (R) and the average absolute relative error (AARE) [13, 15, 25], as expressed in eqs (4) and (5), respectively. The correlation coefficient is a widely used evaluator to measure the strength of linear relationships between experimental and predicted values, while the AARE reflects the accuracy of the prediction. High level of R-values and low level of AARE values indicate that the predicted flow stress values agree very well with the experimental value:

$$R = \frac{\sum_{i=1}^{N}(E_i - \overline{E})(P_i - \overline{P})}{\sqrt{\sum_{i=1}^{N}(E_i - \overline{E})^2 \sum_{i=1}^{N}(P_i - \overline{P})^2}} \tag{4}$$

$$\mathrm{AARE}(\%) = \frac{1}{N}\sum_{i=1}^{N}\left|\frac{E_i - P_i}{E_i}\right| \times 100 \tag{5}$$

where E is the sample of experimental value, P is the sample of predicted value by ANN model, $\overline{E}$ and $\overline{P}$ are the mean value of E and P, respectively, and N is the number of strain–stress samples.

Figure 4(a) and 4(b) shows the correlation relationships of experimental and predicted values for the training procedure and testing procedure, respectively. As shown in Figure 4, the correlation coefficient (R) values for the training procedure and testing procedure were linearly fitted with a value of 0.99998 and 0.99981, respectively. Meanwhile the AARE values for the training procedure and testing procedure were calculated to be determined percent of 0.2947 and 0.5692, respectively. The excellent R-values and AARE values indicate a good correlation between experimental and predicted flow stress values by the ANN model. As a result, the well-trained ANN model has achieved the ideal accuracy and is able to predict the flow behaviors of as-extruded 7075 aluminum alloy well.

As the well-trained ANN model has achieved excellent accuracy, it can be adopted to predict the flow stress in a wide range of temperature, strain and strain rate. Figure 5 shows the comparisons between the datasets predicted by ANN model and the strain–stress curves obtained from compression tests. It is obviously seen in Figure 5 that the predicted datasets fit the experimental curves well in a temperature range of 573–723 K, a strain rate range of 0.01–10 s^{-1}, and a wide strain range of 0.025–0.9.

Generalization capability of ANN model

As stated above, the well-trained ANN model for as-extruded 7075 aluminum alloy is effective in flow

behavior modeling under limited experimental conditions. For the purpose of measuring the generalization capability of the well-trained ANN model for as-extruded 7075 aluminum alloy, several groups of flow stresses in and out of experimental conditions were predicted. Taking the datasets at temperature range of 573–723 K with an interval of 25 K, logarithm strain rate range from −2 to 1 with an interval of 0.5, and strain range from 0.05 to 0.9 with an interval of 0.05 as input data, the corresponding flow stresses were outputted through the well-trained ANN model. Figure 6 shows the true stress–strain curves of as-extruded 7075 aluminum alloy in and out of experimental conditions predicted by the well-trained ANN model. It can be noticed that the predicted stress

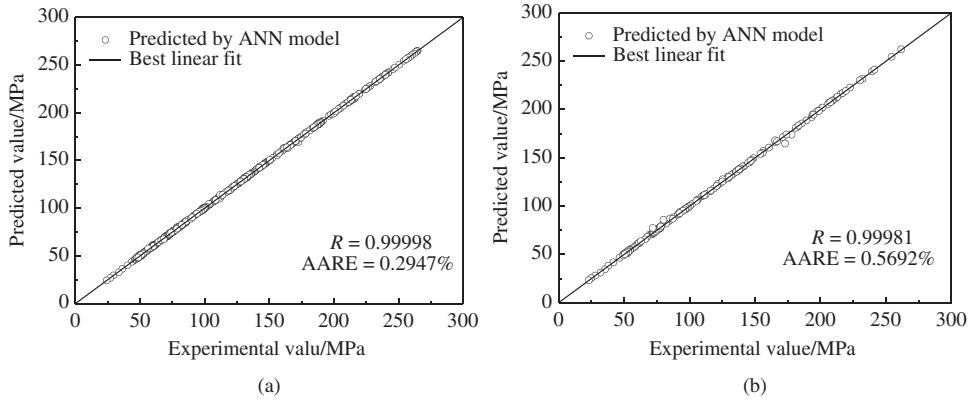

Figure 4: Correlation between experimental and predicted flow stresses for (a) the training procedure and (b) the testing procedure.

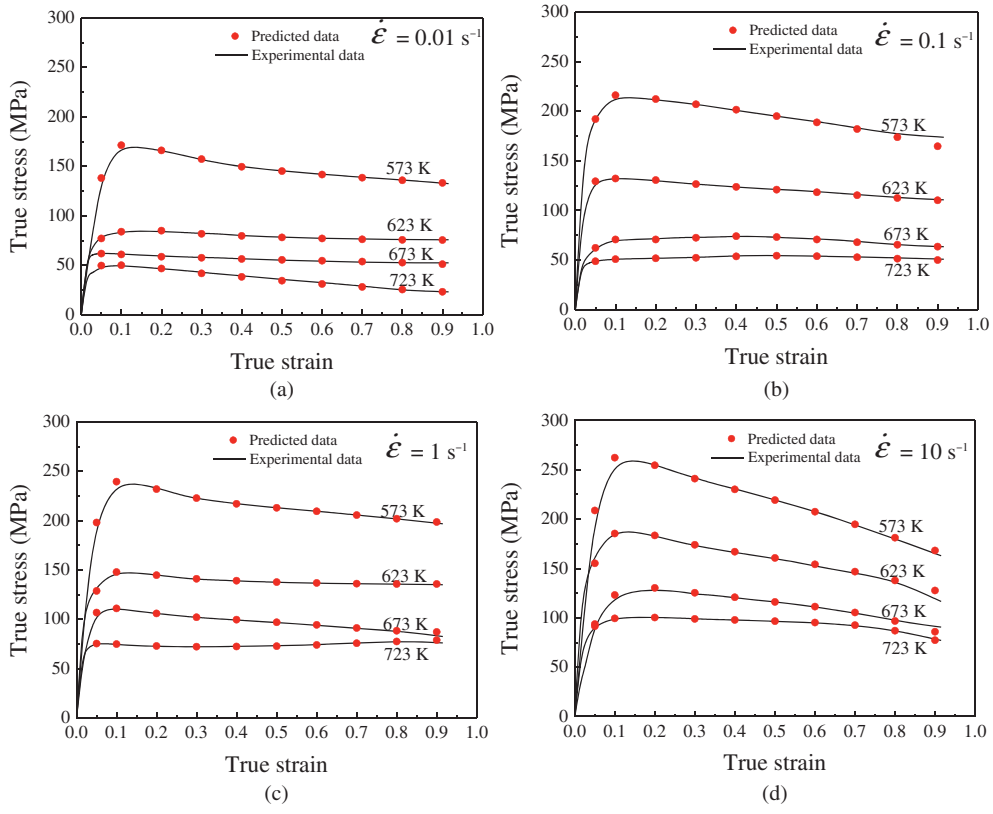

Figure 5: Comparison between the experimental and predicted flow stresses by ANN model at different temperatures and strain rates of (a) 0.01 s^{-1}, (b) 0.1 s^{-1}, (c) 1 s^{-1} and (d) 10 s^{-1}.

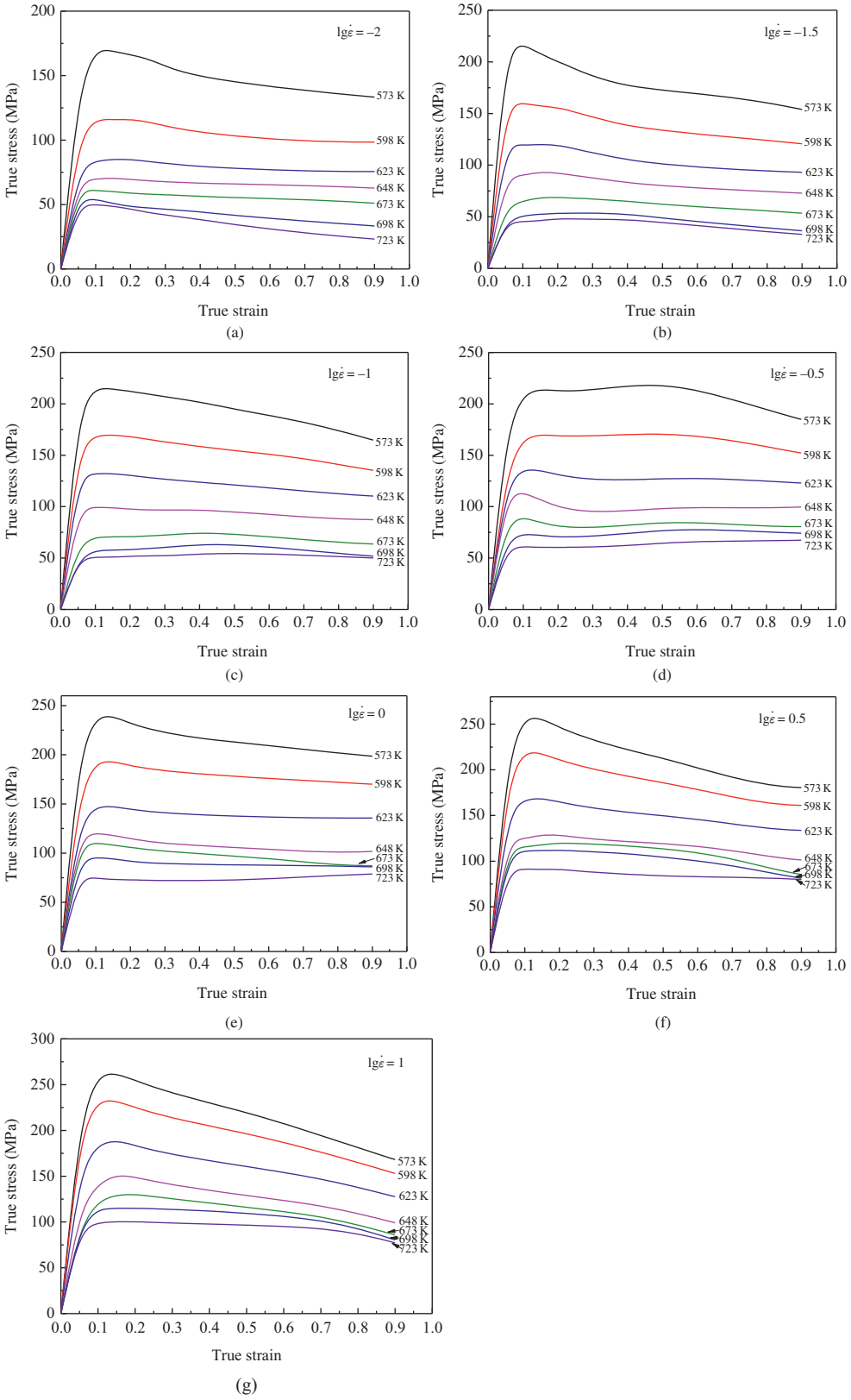

Figure 6: The true stress–strain curves of as-extruded 7075 aluminum alloy in and out of experimental conditions predicted by the well-trained ANN model with logarithm of strain rate (a) −2, (b) −1.5, (c) −1, (d) −0.5, (e) 0, (f) 0.5 and (g) 1.

curves in and out of experimental conditions articulate similar intrinsic characteristics with experimental strain–stress curves. In addition, a 3D plot for the semi-continuous visualized description of the ANN model within the temperature range of 573–723 K, logarithm strain rate ranging from −2 to 1 and strain range from 0.05 to 0.9 were developed, as shown in Figure 7. In Figure 7, the axes of *X*, *Y* and *Z* represent the strain rate in log, temperature and strain, respectively. Meanwhile, the flow stress level was measured in different colors, as shown in the color bar on the right side. The 3D plot visually reflects the variation of flow stresses with the variation of temperature, strain and strain rate. With the increase of strain, the flow stress increases rapidly to a peak value and then decreases monotonically toward a relatively low steady state. Additionally, the increase of strain rate, as well as the decrease of temperature, results in the rise of stress level. The variation of flow stresses matches well with the characteristic of experimental flow curves within the temperature range of 573–723 K, logarithm strain rate ranging from −2 to 1 and strain range from 0.05 to 0.9, which indicates good generalization capability of the well-trained ANN model for as-extruded 7075 aluminum alloy.

Comparison of Arrhenius-type constitutive equation and ANN model for as-extruded 7075 aluminum alloy

Arrhenius-type constitutive equations for as-extruded 7075 aluminum alloy

Traditionally, the Arrhenius-type constitutive equation is expressed as eq. (6) in which the strain is not involved. As mentioned previously, the influence of strain was incorporated in the Arrhenius-type constitutive equation by expressing the hot forming parameters (such as Q, n, a and A) as functions of strain by Lin et al. [20]. The improved Arrhenius-type constitutive equation is expressed as eq. (7). The improved Arrhenius-type constitutive equation of as-extruded 7075 aluminum alloy has been calculated by Quan et al. and reported in

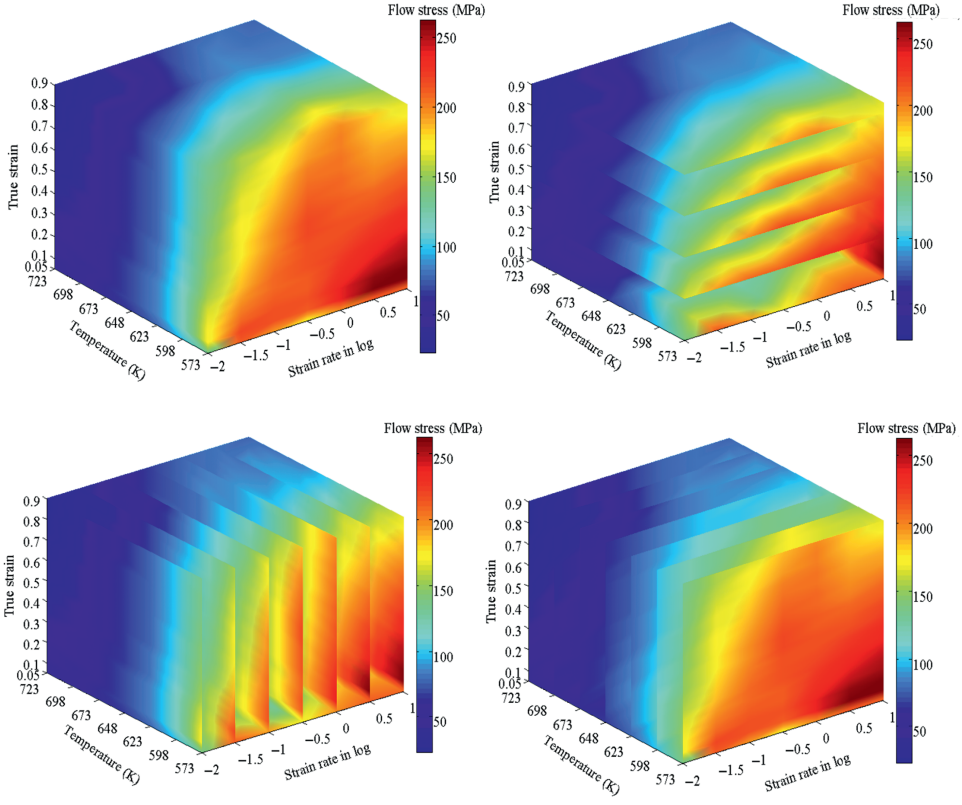

Figure 7: The 3D plot of flow stress within the temperature range of 573–723 K, logarithm strain rate range from −2 to 1 and strain range from 0.05 to 0.9.

Table 1: Polynomial fitting results of Q, n, ln A and α of as-extruded 7075 aluminum alloy.

	Q		n		ln A		α
B_0	119.53	C_0	9.29	D_0	36.74	E_0	0.02
B_1	−90.57	C_1	−32.50	D_1	−120.40	E_1	−0.04
B_2	−466.16	C_2	217.29	D_2	968.02	E_2	−0.17
B_3	2,438.20	C_3	−791.47	D_3	−4,208.20	E_3	1.46
B_4	−3,718.53	C_4	1,539.51	D_4	−8,971.23	E_4	−3.39
B_5	1,916.67	C_5	−1,511.65	D_5	−9,098.29	E_5	3.42
B_6	3.77×10^{-11}	C_6	587.96	D_6	3,537.04	E_6	−1.29

Ref. [17]. In that work, a series of coefficients (Q, n, A and a) were calculated and shown in Table 1:

$$\sigma = \frac{1}{\alpha}\ln\left\{\left(\frac{\dot{\varepsilon}\exp(Q/8.314T)}{A}\right)^{1/n} + \left[\left(\frac{\dot{\varepsilon}\exp(Q/8.314T)}{A}\right)^{2/n} + 1\right]^{1/2}\right\} \quad (6)$$

where σ is the flow stress (MPa) for given strain, $\dot{\varepsilon}$ is the strain rate (s^{-1}), T is the absolute temperature (K), Q is the activation energy of hot deformation (kJ/mol), A, α and n are material constants:

$$\sigma = \frac{1}{g(\varepsilon)}\ln\left\{\left(\frac{\dot{\varepsilon}\exp(j(\varepsilon)/8.314T)}{f(\varepsilon)}\right)^{1/h(\varepsilon)} + \left[\left(\frac{\dot{\varepsilon}\exp(j(\varepsilon)/8.314T)}{f(\varepsilon)}\right)^{2/h(\varepsilon)} + 1\right]^{1/2}\right\}$$

where $f(\varepsilon)$, $g(\varepsilon)$, $h(\varepsilon)$ and $j(\varepsilon)$ are polynomial functions of strain for A, α, n, Q, respectively, with the detailed expressions as follows:

$$Q = j(\varepsilon) = B_0 + B_1\varepsilon + B_2\varepsilon^2 + B_3\varepsilon^3 + B_4\varepsilon^4 + B_5\varepsilon^5 + B_6\varepsilon^6$$
$$n = h(\varepsilon) = C_0 + C_1\varepsilon + C_2\varepsilon^2 + C_3\varepsilon^3 + C_4\varepsilon^4 + C_5\varepsilon^5 + C_6\varepsilon^6$$
$$\ln A = \ln f(\varepsilon) = D_0 + D_1\varepsilon + D_2\varepsilon^2 + D_3\varepsilon^3 + D_4\varepsilon^4 + D_5\varepsilon^5 + D_6\varepsilon^6$$
$$\alpha = g(\varepsilon) = E_0 + E_1\varepsilon + E_2\varepsilon^2 + E_3\varepsilon^3 + E_4\varepsilon^4 + E_5\varepsilon^5 + E_6\varepsilon^6$$

Comparison of the performance of two models

In order to evaluate the performance of the two models, the relative percentage error (η) is introduced to compare various measurements of the relative difference at strain rates of 0.3, 0.5 and 0.7. The relative percentage error (η) is expressed as eq. (8):

$$\eta(\%) = \frac{P_i - E_i}{E_i} \times 100\% \quad (8)$$

where E is the sample of experimental value, P is the sample of predicted value by ANN model and N is the number of strain–stress samples.

The comparison of η -values of the ANN model and the Arrhenius-type constitutive equation at strain of 0.3, 0.5 and 0.7 are shown in Figure 8. It can be demonstrated that the η-values obtained from ANN model vary from −2.70 % to 0.91 %, whereas for the Arrhenius-type constitutive equation, the η-values are in the range from −4.78 % to 5.63 %. Subsequently, the distribution of η-values was analyzed further since the larger range of η-values does not mean the poorer performance. Figure 9(a) and 9(b) shows the distribution of η-values corresponding to the well-trained ANN model and Arrhenius-type constitutive equation, respectively, in which the height of each histogram expresses the relative frequency of each η-level. The two indicators, namely mean value of η-values (μ) and standard deviation (w), are of great significance for evaluating the two distributions. Mean value is an evaluator obtained by dividing the sum of observed values by the number of observations to measure the magnitude of the

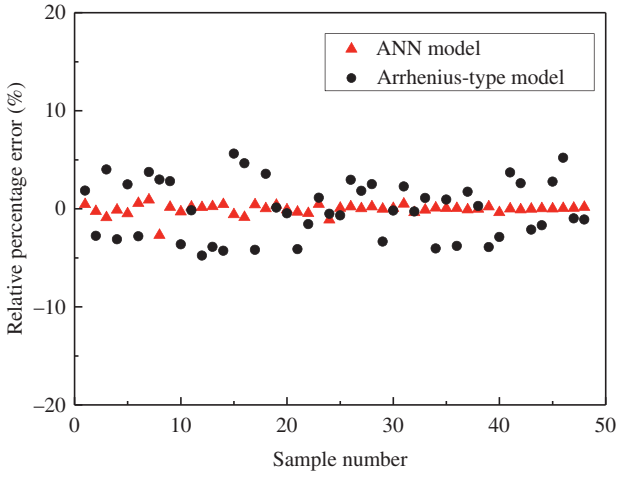

Figure 8: Comparison of relative percent error of predicted value by ANN model and Arrhenius-type constitutive equation with experimental value at strain of 0.3, 0.5 and 0.7.

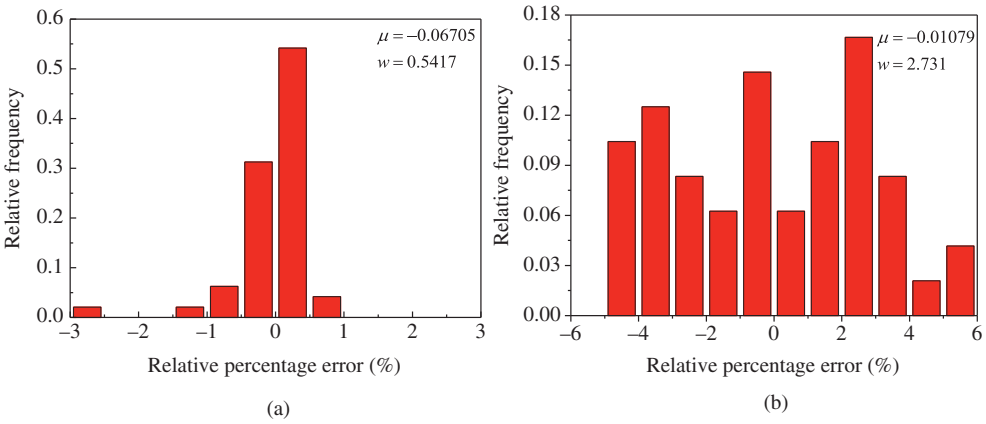

Figure 9: Distribution on relative percentage error by (a) ANN model and (b) Arrhenius-type constitutive equation.

datasets, while standard deviation (w) represents the degree of dispersion and gives an idea of how close the entire set of data is to the average value, as expressed in eqs (9) and (10) [13]:

$$\mu = \frac{1}{N}\sum_{i=1}^{N}\eta_i \tag{9}$$

$$\mathrm{w} = \sqrt{\frac{1}{N-1}\sum_{i=1}^{N}(\eta_i - \mu)^2} \tag{10}$$

where η is the sample of relative percentage error, μ is the mean value of η-values and N is the sample number of relative percentage errors.

Small values of μ and w indicate tightly grouped, precise data. As shown in Figure 9(a) and 9(b), μ-value and w-value of the ANN model are −0.06705 % and 0.5417 %, respectively, compared with the −0.01079 % and 2.731 % from the Arrhenius-type constitutive equation. The μ-value of the two models are both very small, indicating that the predicted stress data by the two models are close to the experimental stress data. However, the w-value of ANN model is much smaller than that of Arrhenius-type constitutive equation, i. e. the ANN model is related to a more centralized distribution of η-values, which means that the ANN model has better reliability and performance than the Arrhenius-type constitutive equation.

Application potentiality of ANN model in hot deformation processes

Processing map

Processing map on the basis of dynamic materials model (DMM) is widely used in the characterization of intrinsic hot workability and optimization of processing parameters for deformation processes such as hot rolling, forging, extrusion, and so on. Generally, the processing map is obtained through the experimental data extracted from the hot isothermal compression test. The limited amount of experimental data may cause a loss of accuracy since interpolation method was employed during the development procedure of processing map. However, with the help of ANN model, reliable processing maps can be constructed in a wider range of strain, strain rate and temperature with minimal experimental work.

In current investigation, a processing map at typical strain of 0.4 was developed with stress data extracted from the ANN model. The power dissipation and instability map were constructed by the calculation of three key indicators in DMM such as strain rate sensitivity (m-value), power dissipation efficiency (η-value) and instability parameter (ξ-value), as shown in Figure 10(a) and 10(b). A superimposition of an instability map on a power dissipation map gives a processing map, in which the stable and unstable regions were clarified clearly. Figure 11(a) and 11(b) shows the processing map at strain of 0.4 based on ANN model and experimental data, respectively. In each processing map, the regions of flow instability marked with “INST” are distinguished from the “safe” domains marked with “Domain” by using thick curves. By avoiding the regions of flow instability and processing under conditions of higher efficiency in the “safe” domains, the intrinsic workability of the material may be optimized and microstructure control may be achieved. It can easily be found in Figure 11(a) that the processing maps based on ANN model at strain of 0.4 exhibit two safe domains. Domain no. 1–0.4 occurs in temperature range from 573 to 660 K and strain rate ranges from 1 to 10 s^{-1} and domain no. 2–0.4 with temperature range from 660 to 723 K and

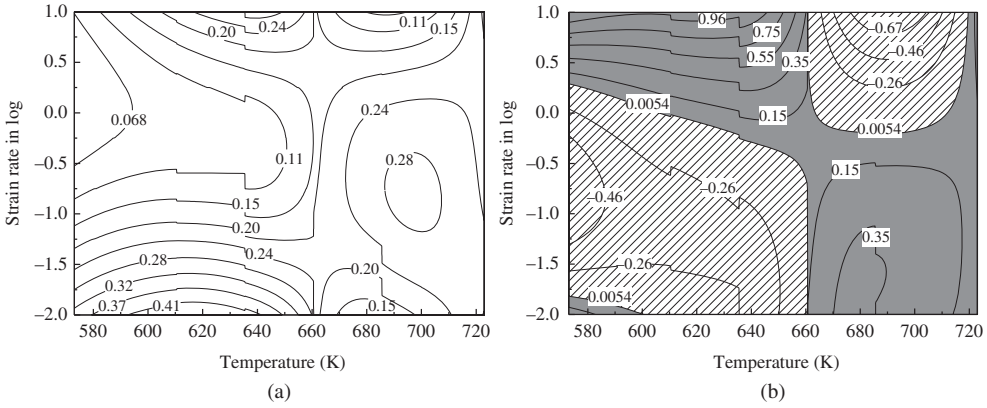

Figure 10: The development of processing map at strain of 0.4 based on ANN model: (a) power dissipation map and (b) instability map.

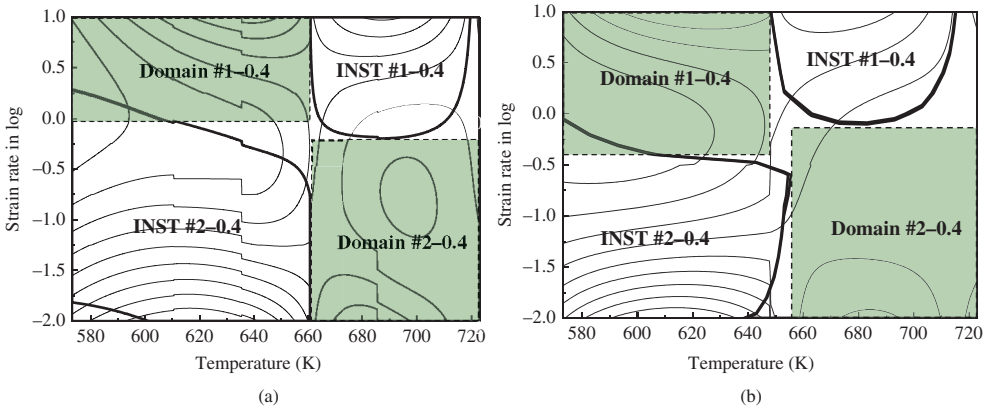

Figure 11: Processing maps based on (a) ANN model and (b) experimental data.

strain rate range from 0.01 to 0.56 s^{-1}. They are similar with the two safe domains in the processing map based on experimental data shown in Figure 11(b) which has been proved to be reliable in Ref. [26], indicating that the processing map based on ANN model is reliable as well. As a result, the processing map based on ANN model is available in the characterization of intrinsic hot workability and optimization of processing parameters for as-extruded 7075 aluminum alloy.

Finite element simulation

As stated earlier, the flow stresses predicted by the well-trained ANN model within the temperature range of 573–723 K, logarithm strain rate range from −2 to 1 and strain range from 0.05 to 0.9 agree very well with the experimental flow stress data. In the current work, the flow stress data extracted from the ANN model were successfully implanted in the finite element analysis software Deform since they were proved to be reliable in flow behaviors modeling of as-extruded 7075 aluminum alloy. In order to demonstrate the reliability of finite element simulation based on predicted flow stress data by ANN model, simulation procedure of isothermal compression test at temperature of 623 K with strain rate of 0.1 s^{-1} was conducted in the software Deform. The top die and bottom die were set as rigid objects, while the billet was set as plastic object, so as to overlook the elastic deformation and reflect the computing method of plastic yielding condition. The thermal radiation and heat exchange between billet and dies surrounding atmosphere was ignored to approximate the actual experimental condition of hot isothermal compression test. Graphite lubricants were used to coat the top and bottom surfaces of specimen during compression test; hence, a shear friction coefficient of 0.1 was chosen to simulate the real friction between the specimens and anvils. In addition, the movement type of top die was set to hydraulic press controlled by constant strain rate.

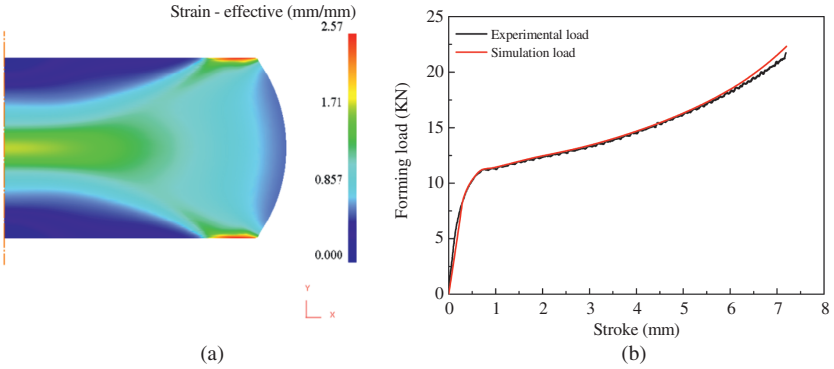

Figure 12: The results of simulation procedure of isothermal compression test: (a) distribution of the effective plastic strain and (b) comparison of forming load between experimental conditions and simulation conditions.

The specimen compressed with a height reduction of 60 % (7.2 mm) was simulated on software Deform, and the results were shown in Figure 12. Figure 12(a) shows the distribution of the effective plastic strain. It can be clearly found from Figure 12(a) that the deformed workpiece is inhomogeneous and can be roughly divided into difficult deformation area, small deformation area and severe deformation area according to the deformation degree. On account of the friction between billet and dies, metal in the vicinity of head face areas is in a state of three-directional compressive stress and difficult to deform. Meanwhile, metal in the heart area undergoes severe deformation due to smaller deformation constraints aroused by friction. In a word, the simulation agrees well with the ideal isothermal compression deformation condition. Figure 12(b) shows the comparison of forming load between experiment condition and simulation condition. As shown in Figure 12(b), the simulation load–stroke curve matches well with the experimental load–stroke curve in the whole deformation stage with similar variation characteristic in which the forming load increases rapidly within the stroke of 1 mm and then reaches a steady increasing state in the last deformation stage. It has been demonstrated that the finite element simulation based on predicted flow stress data by ANN model is effective.

In the hot deformation processes, the material undergoes different strain rates and temperatures, which results in a loss of accuracy in the simulation of typical hot deformation processes with limited amount of experimental flow stress data, since a great number of interpolations have been used in the finite element analysis software. However, with ANN model, more effective flow stresses within different strain rate range and temperature range can be predicted and imported into finite element analysis software. Thus, the span of interpolation is reduced and the accuracy of simulation is improved. In order to demonstrate the higher accuracy of simulation based on predicted flow stress data in the case of typical deformation processes where interpolation methods were adopted automatically in the software, two comparative simulation of isothermal compression tests at the same deformation condition as above with interpolation methods were conducted in the software Deform. The experimental flow stress data at temperature of 573, 673 and 723 K under strain rate of 0.1 were imported in the simulation procedure no. 1, while the predicted flow stress data at temperatures of 573, 598, 648, 673, 698 and 723 K under strain rate of 0.1 were imported in the simulation procedure no. 2. Thus, the flow stress data at temperature of 623 K under strain rate of 0.1 were interpolated automatically in the finite element analysis software during the simulation procedures. Figure 13 shows the load–stroke curves under experiment condition, simulation condition with interpolation of experimental data

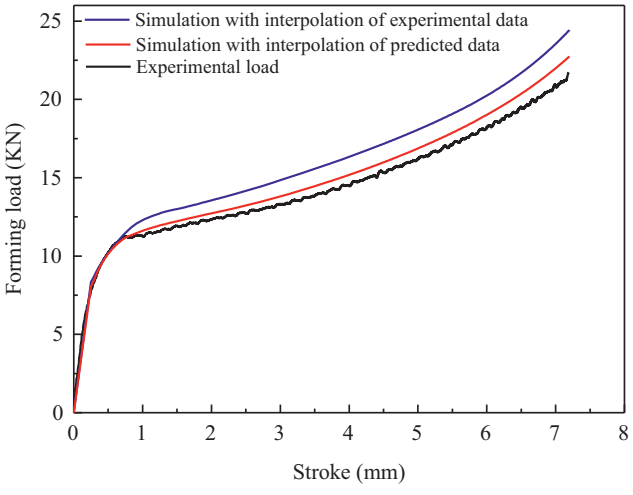

Figure 13: Load–stroke curves under experimental condition, simulation condition with interpolation of experimental data and simulation condition with interpolation of predicted data.

and simulation condition with interpolation of predicted data. It is obvious that the load–stroke curve under simulation condition with interpolation of predicted data is closer to the experimental load–stroke curve than that of simulation condition with interpolation of experimental data, which clearly indicates that the simulation based on predicted flow stress data shows better performance in the case of typical deformation processes where interpolation methods were adopted. In conclusion, the reproducible simulation of the isothermal compression test have illustrated that the well-trained ANN model is available to numerical simulation for the hot deformation behaviors with high accuracy.

Conclusions

An ANN model has been developed to deal with the flow behaviors of as-extruded 7075 aluminum alloy using experimental data from hot compression tests in the temperature range of 573–723 K and strain rate range of 0.01–10 s^{-1}. The following conclusions can be drawn:

(1) The flow stress curves of as-extruded 7075 aluminum alloy show similar characteristics, in which the flow stress increases rapidly to a peak value with the increasing of strain on account of WH and decreases monotonically toward a steady-state region with a varying softening rate which typically indicates the onset of DRX.

(2) The ANN model with BP algorithm for as-extruded 7075 aluminum alloy has been developed on the basis of the experimental data extracted from the isothermal compression tests on Gleeble 1500 thermal simulator. The constructed ANN model is effective in modeling of complex hot deformation behaviors and has excellent generalization capability in a wide temperature range and strain rate range.

(3) A comparative study on Arrhenius-type constitutive equation and ANN model for as-extruded 7075 aluminum alloy was conducted. Higher *R*-value, lower AARE value and better distribution of relative percentage error indicate a better performance of the ANN model under limited experimental conditions than that of the Arrhenius-type constitutive equation.

(4) The applications of ANN model on the processing map and the finite element simulation have been realized, which show excellent performance. The great results have demonstrated that the ANN model has great application potentiality in the field of hot deformation processes.

Funding: The work was supported by Open Fund Project of State Key Laboratory of Materials Processing and Die & Mould Technology (No.P2014-16)

References

[1] Y.C. Lin, L.T. Li, Y.X. Fu and Y.Q. Jiang, J. Mater. Sci., 47 (2012) 1306–1318.
[2] B. Wilshire and P.J. Scharning, J. Mater. Sci., 43 (2008) 3992–4000.
[3] M. Rajamuthamilselvan and S. Ramanathan, J. Alloys Compd., 509 (2011) 948–952.
[4] P. Choudhury and S. Das, J. Mater. Sci., 40 (2005) 805–807.
[5] C.A.C. Imbert and H.J. McQueen, Mater. Sci. Eng. A, 313 (2001) 88–103.
[6] M. Morakabati, M. Aboutalebi, S. Kheirandish, A. Karimi Taheri and S.M. Abbasic, Intermetallics, 19 (2011) 1399–1404.
[7] K. Wu, G.Q. Liu, B.F. Hu, F. Li, Y.W. Zhang, Y. Tao and J.T. Liu, Mater. Des., 32 (2011) 1872–1879.
[8] D. Samantaray, S. Mandal, A.K. Bhaduri, S. Venugopal and P.V. Sivaprasad, Mater. Sci. Eng. A, 528 (2011) 1937–1943.
[9] Y.C. Zhu, W.D. Zeng, Y. Sun, F. Feng and Y.G. Zhou, Comput. Mater. Sci., 50 (2011) 1785–1790.
[10] H. Sheikh and S. Serajzadeh, J. Mater. Process. Technol., 196 (2008) 115–119.
[11] S. Malinov and W. Sha, Mater. Sci. Eng. A, 365 (2004) 202–211.
[12] Z. Guo, S. Malinov and W. Sha, Comput. Mater. Sci., 32 (2005) 1–12.
[13] G.Z. Quan, W.Q. Lv, Y.P. Mao, Y.W. Zhang and J. Zhou, Mater. Des., 50 (2013) 51–61.
[14] G.Z. Quan, C.T. Yu, Y.Y. Liu and Y.F. Xia, Sci. World J., 2014 (2014) 108492.
[15] Y.C. Lin, J. Zhang and J. Zhong, Comput. Mater. Sci., 43 (2008) 752–758.
[16] J.W. Zhao, H. Ding, W.J. Zhao, M.L. Huang, D.B. Wei and Z.Y. Jiang, Comput. Mater. Sci., 92 (2014) 47–56.
[17] G.Z. Quan, G.S. Li, Y. Wang, W.Q. Lv, C.T. Yu and J. Zhou, Mater. Res., 16 (2013) 19–27.
[18] N.S. Reddy, Y.H. Lee, J.H. Kim and C.S. Lee, Met. Mater. Int., 14 (2008) 213–221.
[19] G.Z. Quan, J.T. Liang, W.Q. Lv, D.S. Wu, Y.Y. Liu, G.C. Luo and J. Zhou, Mater. Res., 17 (2014) 1102–1114.
[20] Y.C. Lin, M.S. Chen and J. Zhang, Mater. Sci. Eng. A, 499 (2009) 88–92.
[21] G.Z. Quan, G.S. Li, T. Chen, Y.X. Wang and Y.W. Zhang, Mater. Sci. Eng. A, 528 (2011) 4643–4651.
[22] P.A. Lucon and R.P. Donovan, Composites Part B, 38 (2007) 817–823.
[23] S.C. Juang, Y.S. Tarng and H.R. Lii, J. Mater. Process. Technol., 75 (1998) 54–62.
[24] R.X. Chai, C. Guo and L. Yu, Mater. Sci. Eng. A, 534 (2012) 101–110.
[25] Y.C. Lin, D.X. Wen, J. Deng, G. Liu and J. Chen, Mater. Des., 59 (2014) 115–123.
[26] G.Z. Quan, Y.X. Wang, T. Chen and J. Zhou, J. Funct. Mater., 42 (2011) 1673–1677.